Offshore-onshore record of Last Glacial Maximum–to–present grounding line retreat at Pine Island Glacier, Antarctica

Keir A. Nichols[1,*], Dylan H. Rood[1], Ryan A. Venturelli[2], Greg Balco[3], Jonathan R. Adams[1,4], Louise Guillaume[1], Seth Campbell[5], Brent M. Goehring[6], Brenda L. Hall[5], Klaus Wilcken[7], John Woodward[8], and Joanne S. Johnson[4]

[1]Department of Earth Science and Engineering, Imperial College London, London, SW7 2BX, UK
[2]Department of Geology and Geological Engineering, Colorado School of Mines, Golden, Colorado 80401, USA
[3]Berkeley Geochronology Center, Berkeley, California 94709, USA
[4]British Antarctic Survey, Cambridge, CB3 0ET, UK
[5]School of Earth and Climate Sciences and the Climate Change Institute, University of Maine, Orono, Maine 04469, USA
[6]Earth and Environmental Sciences Division, Los Alamos National Laboratory, Los Alamos, New Mexico 87544, USA
[7]Australian Nuclear Science and Technology Organisation (ANSTO), Lucas Heights, New South Wales 2234, Australia
[8]Geography and Environmental Sciences, Northumbria University, Newcastle, NE1 8ST, UK

ABSTRACT

Pine Island Glacier, West Antarctica, is the largest Antarctic contributor to global sea-level rise and is vulnerable to rapid retreat, yet our knowledge of its deglacial history since the Last Glacial Maximum is based largely on marine sediments that record a retreat history ending in the early Holocene. Using a suite of [10]Be exposure ages from onshore glacial deposits directly adjacent to Pine Island Glacier, we show that this major glacier thinned rapidly in the early to mid-Holocene. Our results indicate that Pine Island Glacier was at least 690 m thicker than present prior to ca. 8 ka. We infer that the rapid thinning detected at the site farthest downstream records the arrival and stabilization of the retreating grounding line at that site by 8–6 ka. By combining our exposure ages and the marine record, we extend knowledge of Pine Island Glacier retreat both spatially and temporally: to 50 km from the modern grounding line and to the mid-Holocene, providing a data set that is important for future numerical ice-sheet model validation.

INTRODUCTION

Pine Island Glacier is part of the "weak underbelly of the West Antarctic Ice Sheet" due to its reverse-sloping bed situated below sea level and associated susceptibility to rapid retreat (Hughes, 1981). Pine Island Glacier is also Antarctica's largest contributor to sea-level rise and contains enough ice to raise global sea level by 0.5 m (Rignot et al., 2019). The aim of this study is to determine the thinning history of Pine Island Glacier following the Last Glacial Maximum (LGM), when the West Antarctic Ice Sheet (WAIS) was more extensive than it is today. Antarctic ice loss contributes a large source of uncertainty in future sea-level projections (IPCC, 2021), and paleoglaciological reconstructions provide historical constraints against which models can be validated (e.g.,

Keir Nichols https://orcid.org/0000-0002-9447-9918
*keir.nichols@imperial.ac.uk

Whitehouse et al., 2012; Pollard et al., 2017), thus reducing that uncertainty.

Our knowledge of past ice-sheet change in Pine Island Bay and the wider Amundsen Sea Embayment (ASE; Fig. 1) is based on a combination of surface exposure ages and marine geologic evidence. Geologic constraints from the marine environment (Graham et al., 2010; Hillenbrand et al., 2013; Larter et al., 2014) and exposure ages from islands in Pine Island Bay (Lindow et al., 2014; Braddock et al., 2022) show that grounded ice retreated from the shelf edge from 12 to 9 calibrated (cal.) k.y. B.P. and was ~120 km downstream of the modern grounding line by the early Holocene (Larter et al., 2014). Exposure ages from nunataks (Maish Nunatak, Mt. Moses, and Mt. Manthe) in the Hudson Mountains show that Larter Glacier, a tributary of Pine Island Glacier (Fig. 1), was thicker than present at the LGM and thinned rapidly at ca. 7 ka (Johnson et al., 2014), postdating the marine record of rapid grounding line retreat

(12–9 cal. k.y. B.P.), though the exposure ages do not preclude earlier thinning. Rapid inland thinning should theoretically accelerate as the grounding line approaches due to a steepened glacier surface proximal to the grounding line. Thus, without a large change in the accumulation rate, thinning at our inland sites corresponds with a retreating grounding line archived in the marine record. Because of the proximity and association of Larter Glacier to Pine Island Glacier, Johnson et al. (2008, 2014) inferred from their Larter Glacier sites that Pine Island Glacier itself was at least 150 m thicker at the LGM. In this present study, we remove the need to assume the thinning history of this major glacier by presenting exposure ages from sites directly adjacent to this glacier. Reduced buttressing of inland ice through the breakup or weakening of an ice shelf in Pine Island Bay driven by upwelling of warm Circumpolar Deep Water onto the continental shelf is thought to have been a dominant driver of rapid Holocene ice thinning/retreat of Pine Island Glacier (Hillenbrand et al., 2017; Johnson et al., 2014). Relative sea level (RSL) in Pine Island Bay, thought to reflect isostatic rebound following early–mid-Holocene deglaciation, has fallen steadily from ca. 5.5 ka to the present (Braddock et al., 2022).

Here, we present 27 [10]Be exposure ages from glacial deposits on nunataks in the Hudson Mountains, which lie adjacent to Pine Island Glacier (Fig. 1). Our data set, when combined with marine geologic data, can be used to capture the time dependence of thinning associated with grounding line retreat of Pine Island Glacier. We show that this glacier was at least
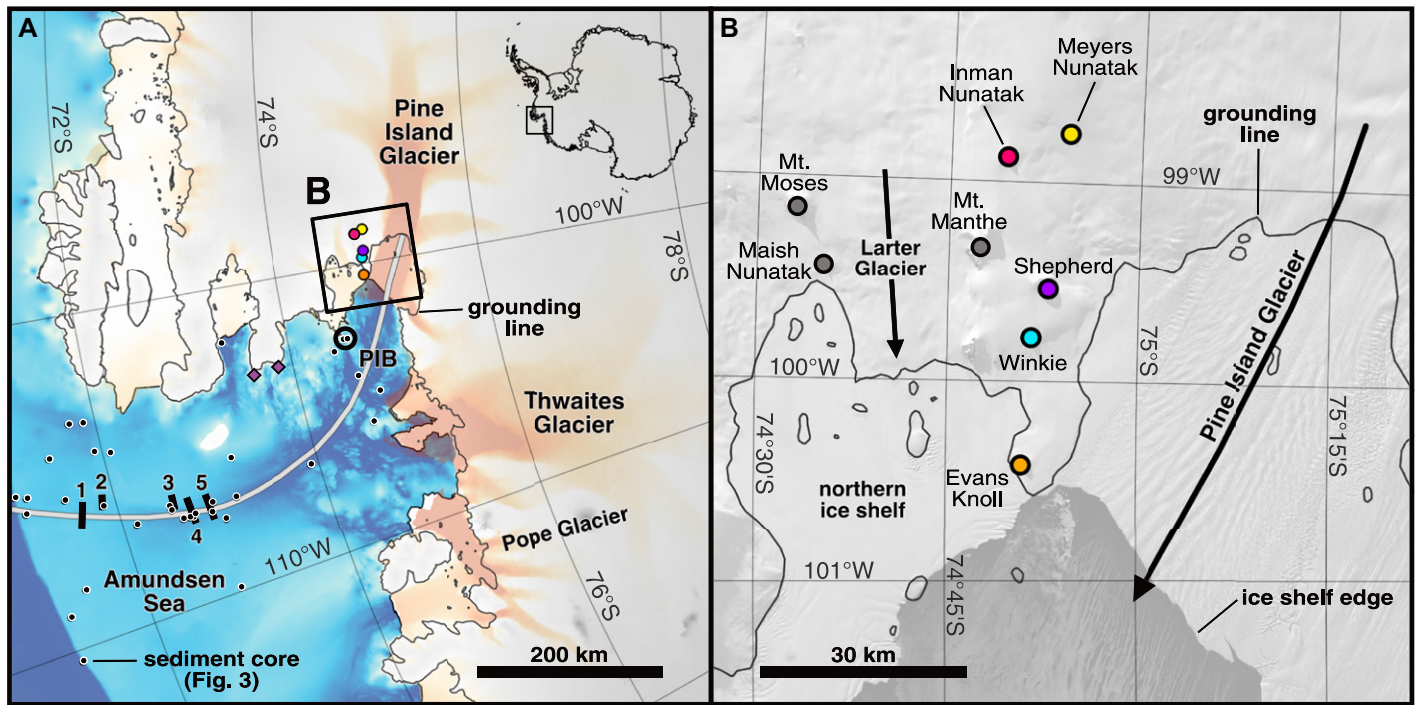
Figure 1. (A) Amundsen Sea sector of the West Antarctic Ice Sheet. Orange shading highlights major ice streams using ice velocities (darker orange is faster ice). Black dots are locations of sediment cores from which radiocarbon ages in Figure 3 and Table S6 (see text footnote 1) were sourced. Black circle shows two nearest sediment cores (PS75/214–1 and PS75/160–1; Hillenbrand et al., 2013) to Pine Island Glacier. Gray line is Pine Island Trough (PIT). Black bars are grounding zone wedges in PIT (see Fig. 3; Graham et al., 2010). Purple diamonds show sampling locations of Braddock et al. (2022). Bathymetry was sourced from BedMachine V2 (Morlighem et al., 2020). Ice velocities and grounding line position were sourced from MEaSUREs program V2 (Rignot et al., 2011, 2017; Mouginot et al., 2012, 2017). PIB—Pine Island Bay. (B) Hudson Mountains. Circles show nunataks sampled for this (colored) and previous studies (gray; Johnson et al., 2008, 2014). Shepherd and Winkie are Shepherd Dome and Winkie Nunatak, respectively. Arrow showing direction of Pine Island Glacier is approximate centerline used in Figure S1 to determine relative sample elevations (see text footnote 1). Copernicus Sentinel satellite imagery is courtesy of European Space Agency. Maps were generated using data sets from Quantarctica V3 (Matsuoka et al., 2021).

690 m thicker at the LGM and thinned rapidly in the early Holocene. Ice at the site farthest downstream thinned first, and this thinning propagated ~50 km through upstream sites. We interpret this pattern of deglaciation as recording the timing of grounding line stabilization adjacent to the site farthest downstream. By combining our exposure ages with marine radiocarbon ages, we extend reconstructions of grounding line retreat developed from onshore and offshore data, recording the end of rapid retreat across the shelf.

METHODS

We collected quartz-bearing (granitic) erratic cobbles from five basaltic nunataks in the Hudson Mountains adjacent to Pine Island Glacier (Fig. 1; Supplemental Material[1]) that lie along

---

[1]Supplemental Material. Detailed description of the methods used in this study, as well as sample locations, analytical data, exposure ages, and linear thinning rates. Exposure ages and analytical data (Tables S1–S3) are also publicly accessible from the UK Polar Data Centre, https://doi.org/10.5285/9ddd50c8-cd08-4afe-b245-f6891f1d9a3f. Please visit https://doi.org/10.1130/GEOL.S.23713422 to access the supplemental material, and contact editing@geosociety.org with any questions.

a 50 km transect broadly parallel to the flow-line of Pine Island Glacier between Evans Knoll and Meyers Nunatak, adjacent to the modern grounding line of the main trunk of Pine Island Glacier (Fig. 1; Fig. S1). Their proximity to Pine Island Glacier means that these erratics were likely deposited by the glacier when it was more extensive during the LGM and hence should yield exposure histories that record when it thinned. There are no granitic outcrops in the Hudson Mountains, indicating that these samples were not transported to the study sites by local ice, but were instead sourced from upstream by an expanded Pine Island Glacier.

We prepared samples for ^{10}Be measurement in the CosmIC Laboratory, Imperial College London (see Supplemental Material), and measured ^{10}Be/^{9}Be ratios at the Centre for Accelerator Science, Australian Nuclear Science and Technology Organisation (ANSTO), using procedures described in Wilcken et al. (2022). Sample information (Table S1), analytical data (Table S2), exposure ages (Table S3), information formatted for online exposure age calculator input (Table S4), thinning rate estimates (Table S5; Jones et al., 2019), and legacy marine radiocarbon data (Table S6) are described in detail in the Supplemental Material.

RESULTS AND DISCUSSION

Our exposure ages all postdate the LGM, ranging from 8.2–7.6 ka at Evans Knoll, 12.4–6.8 at Winkie Nunatak, 7.5–6 ka at Shepherd Dome, 7.3–6.5 ka at Inman Nunatak, and 10.3–6.5 ka at Meyers Nunatak (Fig. 2; Table S2). All but two of the 27 samples analyzed yield ages between 8.2 and 5.9 ka (exceptions being MEY-102 at 10.3 ± 0.8 ka and UNN-106 at 12.4 ± 0.8 ka; Fig. 2). Multiple samples yield Holocene ages from the same or similar elevations as those two samples, with no clear difference in the degree of weathering between any of the samples. We thus infer that the two older samples contain nuclide inheritance. At all sites except Evans Knoll, exposure ages form trends of decreasing age with decreasing elevation, which we interpret as evidence of ice-sheet thinning. At Evans Knoll, there is no discernible difference in exposure age with elevation, suggesting that deglaciation of the entire outcrop occurred ca. 8 ka.

Results from all nunataks (Fig. 2) show that, during the early Holocene, Pine Island Glacier covered surfaces 690 m above the present elevation of the main trunk of the glacier. Additionally, our results show that Pine Island Glacier experienced rapid thinning in the early to mid-
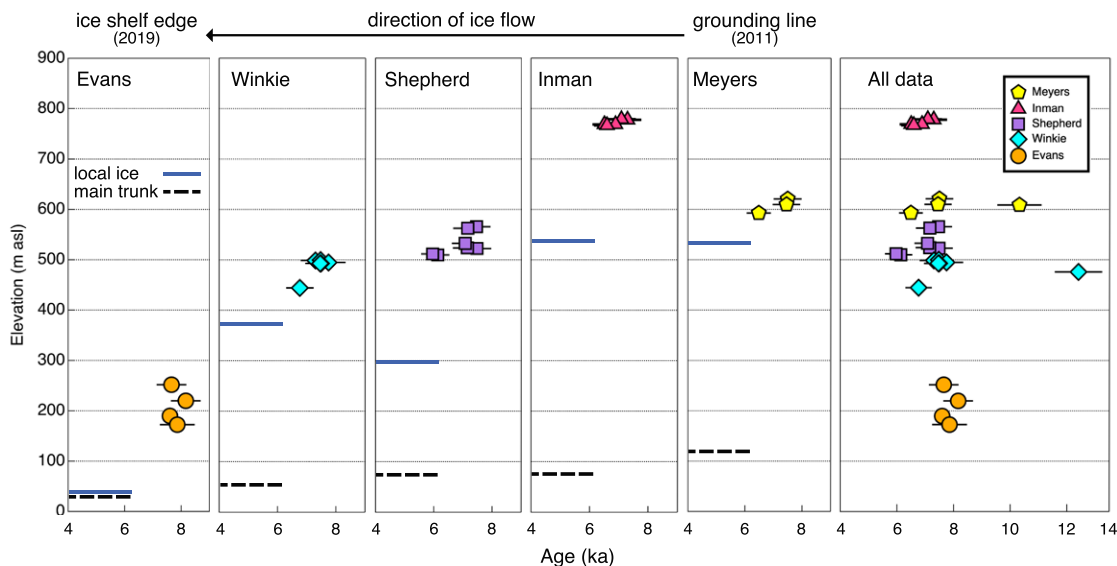
Figure 2. ¹⁰Be exposure ages from nunataks proximal to Pine Island Glacier (PIG; with external uncertainties). Plots are arranged by their location along glacier, from Evans Knoll (farthest downstream) to Meyers Nunatak (farthest upstream). Mean age and standard deviation are plotted for two samples with replicate measurements (EVK-103 and INM-105). Horizontal lines show elevations of surface of main trunk of PIG adjacent to each nunatak (dashed black) and ice margin immediately adjacent to the site (local ice; blue); m asl—m above sea level. See Supplemental Material for ages plotted with these elevations and methods used to define them (text footnote 1).

Holocene, with all sites deglaciating from 8 to 6 ka. By assuming that thinning of the tributaries of Pine Island Glacier would occur simultaneously with thinning of its main trunk, previous work used exposure ages from nunataks adjacent to, and close to, the grounding line of the tributary Larter Glacier to infer the Holocene history of Pine Island Glacier (Fig. 1; Johnson et al., 2014). Our data set builds on these previous results by providing evidence for past rapid thinning of Pine Island Glacier itself, and it extends by almost 300 m the altitudinal range over which we know rapid thinning occurred. Our new exposure ages and those from Pope Glacier (Fig. 1; Johnson et al., 2020; Adams et al., 2022) document that at least two major ice streams in this sector of the ice sheet, Thwaites and Pine Island Glaciers, experienced rapid thinning in the early Holocene. We thereby add to the growing data set recording widespread rapid early to mid-Holocene thinning around the coast of Antarctica (Stone et al., 2003; Jones et al., 2022; Suganuma et al., 2022).

In general, our results show that all study sites deglaciated rapidly (tens to hundreds of meters over an ∼1–2 k.y. episode) in the mid-Holocene. In detail, however, there are differences in both the timing and rate of deglaciation between nunataks. There is a detectable difference between the timing of deglaciation at Evans Knoll (farthest downstream; Fig. 2) and the other nunataks located up to 50 km upstream. Deglaciation took place first at Evans Knoll ca. 8 ka, possibly recording when the grounding line retreated to this location, or at least recording an episode of significant Pine Island Glacier grounding line retreat. In contrast, the upstream sites deglaciated slightly later, from 8 to 6 ka, with no discernible difference in the timing of thinning between nunataks. Further-

more, ice thinned most rapidly at Evans Knoll, where the median estimated thinning rate in the early Holocene is 0.12 m yr⁻¹ (Fig. S4). Early Holocene thinning was more gradual at sites upstream, with median thinning rates ranging from 0.01 to 0.07 m yr⁻¹ (Figs. S5–S8).

The early deglacial history in Pine Island Trough (Fig. 1A) has been reconstructed through several marine geologic studies in the ASE (Fig. 3; e.g., Larter et al., 2014). The oldest, post-LGM radiocarbon ages from sediment cores collected in the ASE (Fig. 1A), which constrain the timing of grounding line retreat, show that the grounding line of Pine Island Glacier reached ∼120 km downstream of the modern grounding line by ca. 11 cal. k.y. B.P. (Smith et al., 2014). We infer that the rapid thinning at

Evans Knoll (ca. 8 ka) and associated slightly later drawdown at upstream sites record the arrival and stabilization of the grounding line adjacent to Evans Knoll. The pattern of thinning may also indicate that ice over the Hudson Mountains reorganized to a more radial configuration during deglaciation, leaving thicker ice for a longer period at upstream sites. We note that these explanations are not mutually exclusive and are consistent with the arrival and stabilization of the grounding line adjacent to Evans Knoll. We present two grounding line histories (Fig. 3) to show that our exposure ages postdate the marine record without relying on the most proximal, oldest radiocarbon age (Hillenbrand et al., 2013). Our inferred timing of grounding line retreat and stabilization
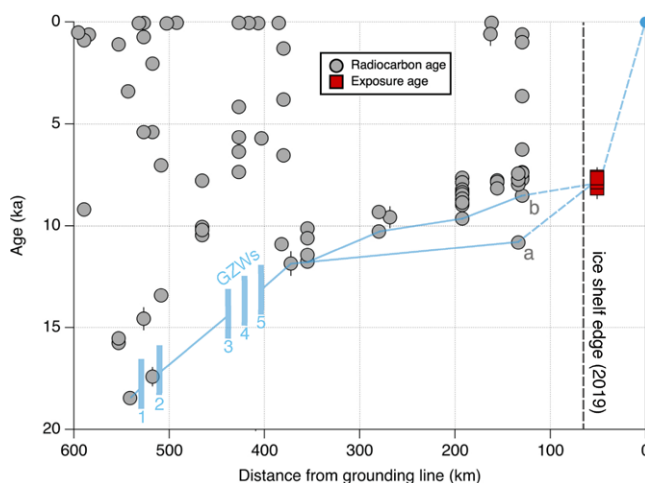

Figure 3. Radiocarbon ages from sediment cores collected from Amundsen Sea Embayment (ASE) proximal to Pine Island Trough (PIT) and ¹⁰Be exposure ages from Evans Knoll. Ages and locations of grounding zone wedges (vertical blue bars labeled GZWs) are projected onto a transect along PIT (see Fig. 1A). Blue lines are estimated grounding line position through time inferred from radiocarbon ages (solid line), which provide minimum ages of ice retreat, and exposure ages (dashed lines). Two grounding line histories were inferred using the oldest ages, labeled a and b, from two sediment cores most proximal to Pine Island Glacier (Fig. 1A, cores PS75/214–1 and PS75/160–1; Hillenbrand et al., 2013). Radiocarbon ages are included in Table S6 (see Supplemental Material for details on age calibration and marine reservoir correction [text footnote 1]). Radiocarbon ages are plotted with 68% confidence intervals; ¹⁰Be ages are plotted with external uncertainties.

Geological Society of America | GEOLOGY | Volume XX | Number XX | www.gsapubs.org

is therefore consistent with the existing marine evidence for the timing of grounding line retreat. Furthermore, our inferred timing of grounding line stabilization, ca. 8 ka, is coincident with the end of deglaciation of the Northern Hemisphere ice sheets (Lambeck et al., 2014; Ullman et al., 2016). We speculate that removal of the influence of melting Northern Hemisphere ice sheets on sea-level rise, combined with RSL fall (driven by glacioisostatic adjustment) in Pine Island Bay taking place by (and likely before) 5.5 ka (Braddock et al., 2022), may have helped stabilize the grounding line at Evans Knoll.

Sometime following stabilization ca. 8 ka, the grounding line of Pine Island Glacier may have retreated inboard of its present position before advancing back toward it (Venturelli et al., 2020, 2023; King et al., 2022). The youngest exposure ages in our data set (ca. 6 ka) leave sufficient time in the late Holocene for Pine Island Glacier to readvance; in other words, the ages are consistent with a Holocene grounding line readvance but cannot provide direct evidence for this advance (Johnson et al., 2022). In contrast, cosmogenic nuclide measurements from bedrock collected from beneath Pope Glacier (Fig. 1) provide direct evidence that ice in the ASE was at least 35 m thinner than present for at least 3 k.y. in the late Holocene (Balco et al., 2023). Such an observation at Pine Island Glacier might appear incompatible with the record of RSL from islands in Pine Island Bay immediately downstream from the modern grounding line of the glacier, which is most easily explained by stability since ca. 5.5 ka (Braddock et al., 2022). However, the late Holocene thinning and associated grounding line retreat may not have been of a large enough magnitude to be expressed in the RSL record.

CONCLUSION

We measured cosmogenic [10]Be in glacially transported cobbles at five nunataks adjacent to Pine Island Glacier to reconstruct past changes in the thickness of this major Antarctic glacier. Our results revealed that Pine Island Glacier was at least 690 m thicker than present prior to ca. 8 ka and subsequently thinned by tens of meters between ca. 8 and 6 ka across a distance of at least ~50 km upstream of the present ice-shelf margin. This thinning was extremely rapid. By inferring that rapid thinning at the site farthest downstream and delayed upstream thinning recorded the arrival of the grounding line adjacent to our study sites, we extend our knowledge of the evolution of the Pine Island Glacier grounding line into the early to mid-Holocene and to within ~50 km of the modern grounding line.

REFERENCES CITED
Adams, J.R., et al., 2022, New [10]Be exposure ages improve Holocene ice sheet thinning history near the grounding line of Pope Glacier, Antarctica: The Cryosphere, v. 16, p. 4887–4905, https://doi.org/10.5194/tc-16-4887-2022.

Balco, G., et al., 2023, Reversible ice sheet thinning in the Amundsen Sea Embayment during the late Holocene: The Cryosphere Discussion, v. 17, p. 1787–1801, https://doi.org/10.5194/tc-17-1787-2023

Braddock, S., Hall, B.L., Johnson, J.S., Balco, G., Spoth, M., Whitehouse, P.L., Campbell, S., Goehring, B.M., Rood, D.H., and Woodward, J., 2022, Relative sea-level data preclude major late Holocene ice-mass change in Pine Island Bay: Nature Geoscience, v. 15, p. 568–572, https://doi.org/10.1038/s41561-022-00961-y.

Graham, A.G.C., Larter, R.D., Gohl, K., Dowdeswell, J.A., Hillenbrand, C.D., Smith, J.A., Evans, J., Kuhn, G., and Deen, T., 2010, Flow and retreat of the late Quaternary Pine Island–Thwaites palaeo-ice stream, West Antarctica: Journal of Geophysical Research: Earth Surface, v. 115, F03025, https://doi.org/10.1029/2009JF001482.

Hillenbrand, C.D., et al., 2013, Grounding-line retreat of the West Antarctic Ice Sheet from inner Pine Island Bay: Geology, v. 41, p. 35–38, https://doi.org/10.1130/G33469.1.

Hillenbrand, C.D., et al., 2017, West Antarctic Ice Sheet retreat driven by Holocene warm water incursions: Nature, v. 547, p. 43–48, https://doi.org/10.1038/nature22995.

Hughes, T.J., 1981, The weak underbelly of the West Antarctic ice sheet: Journal of Glaciology, v. 27, p. 518–525, https://doi.org/10.3189/S002214300001159X.

Intergovernmental Panel on Climate Change (IPCC), 2021, Climate Change 2021—The Physical Science Basis, Contribution of Working Group I to the Sixth Assessment Report of the Intergovernmental Panel on Climate Change: New York, Cambridge University Press, 2391 p., https://doi.org/10.1017/9781009157896.

Johnson, J.S., Bentley, M.J., and Gohl, K., 2008, First exposure ages from the Amundsen Sea Embayment, West Antarctica: The late Quaternary context for recent thinning of Pine Island, Smith, and Pope Glaciers: Geology, v. 36, p. 223–226, https://doi.org/10.1130/G24207A.1.

Johnson, J.S., Bentley, M.J., Smith, J.A., Finkel, R.C., Rood, D.H., Gohl, K., Balco, G., Larter, R.D., and Schaefer, J.M., 2014, Rapid thinning of Pine Island Glacier in the early Holocene: Science, v. 343, p. 999–1001, https://doi.org/10.1126/science.1247385.

Johnson, J.S., et al., 2020, Deglaciation of Pope Glacier implies widespread early Holocene ice sheet thinning in the Amundsen Sea sector of Antarctica: Earth and Planetary Science Letters, v. 548, https://doi.org/10.1016/j.epsl.2020.116501; corrigendum available at https://doi.org/10.1016/j.epsl.2021.117221.

Johnson, J.S., et al., 2022, Review article: Existing and potential evidence for Holocene grounding line retreat and readvance in Antarctica: The Cryosphere, v. 16, p. 1543–1562, https://doi.org/10.5194/tc-16-1543-2022.

Jones, R.S., Small, D., Cahill, N., Bentley, M.J., and Whitehouse, P.L., 2019, iceTEA: Tools for plotting and analysing cosmogenic-nuclide surface-exposure data from former ice margins: Quaternary Geochronology, v. 51, p. 72–86, https://doi.org/10.1016/j.quageo.2019.01.001.

Jones, R.S., Johnson, J.S., Lin, Y., Mackintosh, A.N., Sefton, J.P., Smith, J.A., Thomas, E.R., and Whitehouse, P.L., 2022, Stability of the Antarctic Ice Sheet during the pre-industrial Holocene: Nature Reviews–Earth & Environment, v. 3, p. 500–515, https://doi.org/10.1038/s43017-022-00309-5.

King, M.A., Watson, C.S., and White, D., 2022, GPS rates of vertical bedrock motion suggest late Holocene ice-sheet readvance in a critical sector of East Antarctica: Geophysical Research Letters, v. 49, https://doi.org/10.1029/2021GL097232.

Lambeck, K., Rouby, H., Purcell, A., Sun, Y., and Sambridge, M., 2014, Sea level and global ice volumes from the Last Glacial Maximum to the Holocene: Proceedings of the National Academy of Sciences of the United States of America, v. 111, p. 15,296–15,303, https://doi.org/10.1073/pnas.1411762111.

Larter, R.D., et al., 2014, Reconstruction of changes in the Amundsen Sea and Bellingshausen Sea sector of the West Antarctic Ice Sheet since the Last Glacial Maximum: Quaternary Science Reviews, v. 100, p. 55–86, https://doi.org/10.1016/j.quascirev.2013.10.016.

Lindow, J., Castex, M., Wittmann, H., Johnson, J.S., Lisker, F., Gohl, K., and Spiegel, C., 2014, Glacial retreat in the Amundsen Sea sector, West Antarctica—First cosmogenic evidence from central Pine Island Bay and the Kohler Range: Quaternary Science Reviews, v. 98, p. 166–173, https://doi.org/10.1016/j.quascirev.2014.05.010.

Matsuoka, K., et al., 2021, Quantarctica [Data Set]: Tromsø, Norway, Norwegian Polar Institute, https://doi.org/10.21334/npolar.2018.8516e961.

Morlighem, M., et al., 2020, Deep glacial troughs and stabilizing ridges unveiled beneath the margins of the Antarctic Ice Sheet: Nature Geoscience, v. 13, p. 132–137, https://doi.org/10.1038/s41561-019-0510-8.

Mouginot, J., Scheuchl, B., and Rignot, E., 2012, Mapping of ice motion in Antarctica using synthetic-aperture radar data: Remote Sensing, v. 4, p. 2753–2767, https://doi.org/10.3390/rs4092753.

Mouginot, J., Rignot, E., Scheuchl, B., and Millan, R., 2017, Comprehensive annual ice sheet velocity mapping using Landsat-8, Sentinel-1, and RADARSAT-2 data: Remote Sensing, v. 9, no. 4, 364, https://doi.org/10.3390/rs9040364.

Pollard, D., Gomez, N., and DeConto, R.M., 2017, Variations of the Antarctic Ice Sheet in a coupled ice sheet–earth–sea level model: Sensitivity to viscoelastic Earth properties: Journal of Geophysical Research: Earth Surface, v. 122, p. 2124–2138, https://doi.org/10.1002/2017JF004371.

Rignot, E., Mouginot, J., and Scheuchl, B., 2011, Ice flow of the Antarctic Ice Sheet: Science, v. 333,

p. 1427–1430, https://doi.org/10.1126/science .1208336.

Rignot, E., Mouginot, J., and Scheuchl, B., 2017, MEaSUREs InSAR-Based Antarctica Ice Velocity Map, Version 2 [Data Set]: Boulder, Colorado, National Aeronautics and Space Administration (NASA) National Snow and Ice Data Center Distributed Active Archive Center, https://doi .org/10.5067/D7GK8F5J8M8R (accessed April 2023).

Rignot, E., Mouginot, J., Scheuchl, B., van den Broeke, M., van Wessem, M.J., and Morlighem, M., 2019, Four decades of Antarctic Ice Sheet mass balance from 1979–2017: Proceedings of the National Academy of Sciences of the United States of America, v. 116, p. 1095–1103, https:// doi.org/10.1073/pnas.1812883116.

Smith, J.A., Hillenbrand, C.D., Kuhn, G., Klages, J.P., Graham, A.G.C., Larter, R.D., Ehrmann, W., Moreton, S.G., Wiers, S., and Frederichs, T., 2014, New constraints on the timing of West Antarctic Ice Sheet retreat in the eastern Amundsen Sea since the Last Glacial Maximum: Global and Planetary Change, v. 122, p. 224–237, https://doi .org/10.1016/j.gloplacha.2014.07.015.

Stone, J.O., Balco, G.A., Sugden, D.E., Caffee, M.W., Sass, L.C., Cowdery, S.G., and Siddoway, C., 2003, Holocene deglaciation of Marie Byrd Land, West Antarctica: Science, v. 299, p. 99– 102, https://doi.org/10.1126/science.1077998.

Suganuma, Y., et al., 2022, Regional sea-level high-stand triggered Holocene ice sheet thinning across coastal Dronning Maud Land, East Antarctica: Communications Earth & Environment, v. 3, 273, https://doi.org/10.1038/s43247-022 -00599-z.

Ullman, D.J., Carlson, A.E., Hostetler, S.W., Clark, P.U., Cuzzone, J., Milne, G.A., Winsor, K., and Caffee, M., 2016, Final Laurentide ice-sheet deglaciation and Holocene climate–sea level change: Quaternary Science Reviews, v. 152, p. 49–59, https://doi.org/10.1016/j.quascirev .2016.09.014.

Venturelli, R.A., Siegfried, M.R., Roush, K.A., Li, W., Burnett, J., Zook, R., Fricker, H.A., Priscu, J.C., Leventer, A., and Rosenheim, B.E., 2020, Mid-Holocene grounding line retreat and readvance at Whillans ice stream, West Antarctica: Geophysical Research Letters, v. 47, https://doi .org/10.1029/2020GL088476.

Venturelli, R.A., Boehman, B., Davis, C.L., Hawkings, J.R., Johnston, S.E., Gustafson, C.D., Michaud, A.B., Mosbeux, C., Siegfried, M.R., Vick-Majors, T.J., Galy, V., Spencer, R.G.M., Warny, S., Christner, B.C., Fricker, H.A., Harwood, D.M., Leventer, A., Priscu, J.C., Rosenheim, B.E., and SALSA Science Team, 2023, Constraints on the timing and extent of deglacial grounding line retreat in West Antarctica from subglacial sediments: AGU Advances, v. 4, no. 2, https://doi.org /10.1029/2022AV000846.

Whitehouse, P.L., Bentley, M.J., and Le Brocq, A.M., 2012, A deglacial model for Antarctica: Geological constraints and glaciological modelling as a basis for a new model of Antarctic glacial isostatic adjustment: Quaternary Science Reviews, v. 32, p. 1–24, https://doi.org/10.1016/j.quascirev.2011.11.016.

Wilcken, K.M., Codilean, A.T., Fülöp, R.H., Kotevski, S., Rood, A.H., Rood, D.H., Seal, A.J., and Simon, K., 2022, Technical note: Accelerator mass spectrometry of ^{10}Be and ^{26}Al at low nuclide concentrations: Geochronology, v. 4, p. 339–352, https://doi.org/10.5194/gchron-4-339-2022.

Printed in the USA